Performance of a Large Scale, Nonequilibrium MHD Generator with Rare Gases

B. ZAUDERER* AND E. TATE†
General Electric Company, King of Prussia, Pa.

An experimental study was performed of the operating characteristics of a shock-tunnel driven, supersonic MHD generator. The following major results were obtained: 1) Uniform preionization was required at the generator entrance to achieve appreciable generator power output. 2) The open circuit, induced voltages were in good agreement with the theory. 3) The electrical characteristics and plasma properties of the loaded, Faraday generator were in agreement with the predictions of the one dimensional electron conservation equations, and Ohm's law if the conductivity was computed on the assumption that the plasma was homogeneously turbulent. 4) When the slope of the axial velocity and pressure gradients changed signs, a nonstationary shock-wave formed in the generator which led to boundary-layer separation and eventual generator current cutoff. 5) The maximum generator power of 500 kw was equal to 7½% of the thermal power input. 6) The electrical performance of the present generator was similar to that measured in a generator having 2% of the volume of the present generator. It is concluded that electrode conduction losses and shock-wave formations were the two major factors limiting the efficiency of this generator.

1. Introduction

THIS paper reports on one major phase of a continuing experimental study of the technical feasibility and operating characteristics of the linear, nonequilibrium MHD generator. Previous investigations[1-4] were performed in a small shock-tube driven MHD generator whose volume was 5 cm × 5 cm × 30 cm. The test gases were noble gas mixtures which were shock heated to static gas temperatures of 2500 to 8000°K and a flow Mach number 1.3. It was shown that the electron density of the gas was approximately in Saha equilibrium at the electron temperature,[1] that the electron temperature exceeded the gas stagnation temperature,[1] that the discharge structure in the generator was nonuniform and it was controlled by gas dynamic effects,[2] that the generator operated in the "normal" mode (in which the current, velocity, and magnetic field vectors are orthogonal),[3] and that the effective Hall parameter saturated at a value of about two.[3] The purpose of the present study was to investigate the generator operation under conditions of large scale power extraction and strong electromagnetic-gas dynamic interactions. An additional objective was the determination of the effect of scaling the channel size on the generator performance. The small shock tube was unsuitable for this study because its test time was too short. Therefore, the gas flow was nonsteady in the presence of strong Lorentz forces.[4] Also, in an incident shock tube flow the boundary layer is nonsteady; and it does not correspond to a steady-state, MHD generator boundary layer. Thus, for the present study a large (30 cm-diam., 15 m-long) shock-tunnel was used to drive a supersonic MHD channel. The advantages of the shock tunnel are that the boundary-layer is time independent and that the gas flow time through the generator is short (≈10%) compared to the total available test time of 4 msec. The hot stationary gas behind the reflected shock-wave was used as the generator working fluid. Gas stagnation temperatures and pressures ranged from 2000 to 6000°K and 1 to 10 atm pressure, respectively. A supersonic nozzle expanded the flow to about Mach 1.5 at the generator entrance. The thermal power of the gas ranged from 5 to 50 Mw and the mass flow rate from 1 to 10 kg/sec. Figure 1 shows a top and side view of the MHD channel test section. The figure gives the pertinent channel dimensions, and it shows the locations of the various instrumentation ports and of the electrodes. A full description of the facility is given elsewhere.[5] The generator diagnostics consisted of measurements of the individual preionization and electrode currents, the electric potential distribution on the insulator wall, the static and stagnation pressures in the generator, and the continuum radiation from which the electron density was obtained. In addition, the stagnation pressure and temperature behind the reflected shock-wave in the driven tube were measured. The diagnostic method is described in Ref. 6, which also contains a more detailed description of the present study.

There have been a considerable number of experimental studies of the nonequilibrium, linear MHD generator. The results of many of these studies are summarized in a recent article which surveys the field and lists all the existing facilities.[7] Of these facilities, only one[8] was operated under conditions similar to that in the present experiments; namely, strong electromagnetic-gas dynamic interactions. A supersonic MHD channel was used in that study with cesium-seeded helium at 2000°K as the test gas. The generator was subject to severe internal shorting, and less than 1% of the thermal gas power was extracted as electrical power to the external loads.[8] Further comparison with the results of this experiment will be given in the body of the paper. The other facilities[7] were either too small to operate under conditions of large electromagnetic interactions, or they are still in the initial construction or testing stages.

Received February 27, 1970; revision received December 9, 1970. The authors wish to thank H. Sharp and W. Frey for their assistance in the conduct of these experiments, and V. Kirk for performing the numerical analyses of the theory. This work was supported in part by the Office of Naval Research.

* Manager, MHD Programs, Space Sciences Laboratory. Associate Fellow AIAA.

† Physicist, MHD.

2. MHD Generator Analyses

The purpose of the theoretical analyses was to determine the simplest model which would describe the over-all MHD generator performance and which would identify the parameters limiting the generator power output. A time-independent,

one-dimensional formulation of the electron and total gas conservation equations and Ohm's law was used. Conservation equations similar to those given by Bertolini, Toschi, and McNab[9] were used. For the present analyses the following modifications were made: the electron momentum equation was eliminated based on the assumption that the average Hall current was approximately zero. Based on Bertolini's results, it was assumed that the electron temperature relaxes instantaneously compared to the rate of change of the other dependent variables in the electron energy equation. Also, the electron pressure gradients and the radiation loss were neglected in the electron energy equation. The electron conservation equations were solved simultaneously with the total gas conservation equations for the inviscid core flow, using the Runga-Kutta technique. The effect of the turbulent boundary layer was obtained by simultaneously solving, with the conservation equations, the von Kármán momentum integral equation for the momentum thickness. From the momentum thickness, the boundary layer displacement thickness was obtained. The displacement thickness, which was less than 5% of the channel half-height, was subtracted from the channel cross section to obtain the local inviscid core flow area. Since the preceding formulation is straight forward, the equations are not presented. They can be found in Ref. 6. However, the formulation of Ohm's law used in the present analyses requires further elaboration.

The formulation of Ohm's law for a Faraday MHD generator depends on whether the generator operates in the "normal" mode (in which the current **J**; the field, **B**; and the velocity, **U**, are mutually orthogonal) or in the "shorted" mode (in which **J** is approximately parallel to **U**). Ohm's law for a segmented electrode Faraday generator operating in the "normal" mode is given by

$$j_y = \sigma_{\text{EFF}}(E_y - U_x B_z); \quad E_x = \beta_{\text{EFF}}(E_y - U_x B_z) \quad (1)$$

where j_y and E_y are the transverse current and field, respectively; E_x is the axial Hall field; and σ_{EFF} and β_{EFF} are the effective conductivity and Hall parameters. E_y is the sum of the fields due to the external load and due to the electrode voltage loss. In the Faraday generator the axial, Hall current, j_x, is zero. Equation (1) is coupled to the electron energy equation by the ohmic dissipation term, $(\mathbf{J}\cdot\mathbf{J})/\sigma_{\text{EFF}}$. For an infinitesmally segmented electrode generator having a uniform, nonequilibrium plasma, σ_{EFF} and β_{EFF} in Eq. (1) are given by the scalar conductivity, σ, and the Hall parameter, β. (The method of computing σ is given in Ref. 10.) The infinitesmally segmented electrode generator represents the upper limit of generator performance, and it will be referred to as the "ideal" conductivity model in subsequent discussions.

The use of a finite electrode segmentation ratio, ρ_i, which equaled 0.1 in the present channel, reduces σ_{EFF} and β_{EFF} even if the plasma is uniform. The appropriate expressions for the two parameters are[3]

$$\sigma_{\text{EFF}} = \sigma/[1 + \rho_i(\beta - 0.4)] \quad (2)$$

$$\beta_{\text{EFF}} = \beta/[1 + \rho_i(\beta - 0.4)] \quad (3)$$

As was noted in the Introduction, in previous experiments[2] it was observed that the plasma structure in the generator was nonuniform. A rigorous theoretical formulation of the nonuniform plasma properties in the generator is very complex.[3] It was observed[3] that a reasonably good (within a factor of two) empirical fit of the data could be obtained if the l.h.s. of Eq. 2 was used in the electron energy equation to approximate the increased ohmic dissipation due to plasma nonuniformities. This semi-empirical method will be identified as the "finite electrode" conductivity model.

Another simplified method[11] of computing the effect of plasma nonuniformities is based on the assumptions that the plasma is homogeneously turbulent and that the electrodes are infinitesmally segmented. These two assumptions are

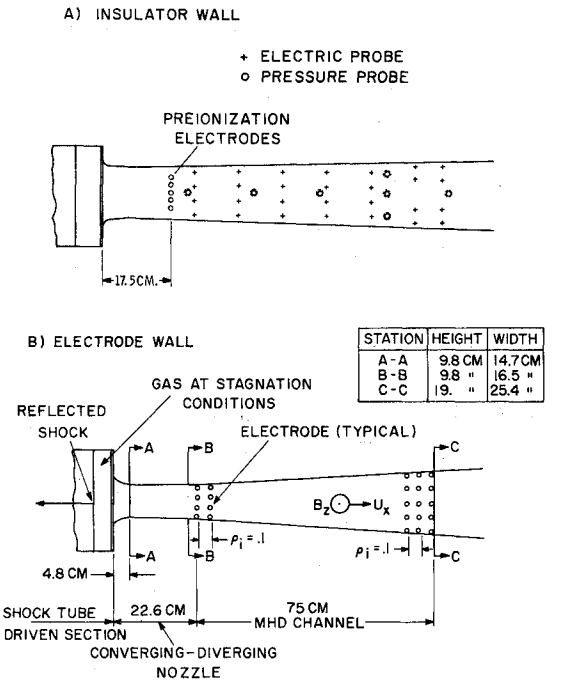

Fig. 1 Schematic of the insulator and electrode walls of the MHD channel. The nozzle throat is at station *A-A*, the generator entrance at *B-B*, and the exit at *C-C*. The 7 pairs of preionization electrodes are oriented parallel to the magnetic field direction. The pulsed magnetic field decreased linearly from 1.38 Tesla at the generator entrance to 1.06 Tesla at the exit. Its magnitude also decreased 17 percent during the 4 msec test time. There are 37 rows of electrodes on each of the two electrode walls. The number of electrodes per row increased uniformly from 4 at the generator entrance to 8 at the exit. The total number of electrode pairs was 230. Each electrode consists of a 0.32 cm-diam copper rod which was flush mounted in the fiberglass channel wall. The axial electrode segmentation ratio, ρ_i, was 0.1. Figure 1a shows the location of 5 pairs of instrumentation ports on the two insulator walls for pressure and optical measurements and 24 electrostatic potential probes.

reasonable since it was observed[2] that the wavelength of the plasma nonuniformities was about 2 cm compared to the average channel width of about 20 cm. Also, the electrode segmentation effect for ρ_i of 0.1 is small if $\beta < 10$. The uniform plasma turbulence derivation shows that when electron-atom collisions are dominant, σ_{EFF} and β_{EFF} are given by[11]

$$\sigma_{\text{EFF}} = \sigma[(\beta - \xi)^2 + \beta^2\xi^2]/\beta[\beta + \xi(\beta^2 - 1)] \quad (4)$$

$$\beta_{\text{EFF}} = \beta(\beta - 2\xi)/[\beta + \xi(\beta^2 - 1)] \quad (5)$$

when ξ is the turbulent fluctuation parameter. For sinusoidal fluctuations, ξ has a maximum of 0.5 and for square waves ξ has a maximum of 1. This model will be referred to as the "plasma turbulence" conductivity model. It is to be noted that in the computations of the "ideal," "finite electrode," or "plasma turbulence" models, the measured j_y was used as an input quantity in the calculations. Alternately, one could use E_y as input and compute j_y. The former method was used because it simplified the numerical analyses.

The above three models of generator operation assume that the generator operates in the "normal" mode. If the generator is internally shorted, as was the case in the experiment cited in Ref. 8, a large Hall current, j_x, flows in the generator. When the generator operates in this "shorted" mode, the net generator power output is essentially zero.[8] The rigorous computation of the "shorted" case is quite complex.[12] A very simplified model was adopted to determine its existence in the present experiments. Since $j_x \neq 0$, Ohm's law [Eq.

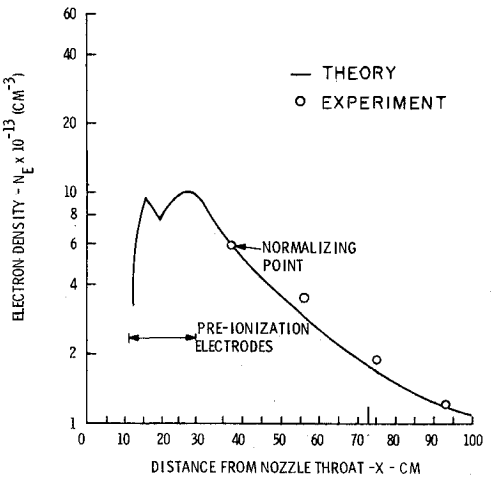

Fig. 2 Axial electron density distribution for the preionization experiment at zero magnetic field in the 99% Ne + 1% Xe mixture. T_o was equal to 3950° k and P_o equalled 1.8 atm. All the data points were normalized to the point indicated in the figure at x = 37 cm. The theoretical curve was computed with Dugan's[13] three body recombination coefficient.

(1)] was replaced by the more general expression

$$j_y = \sigma(E_y - U_x B_z) + \beta j_y \quad (6)$$

$$j_x = \sigma E_x - \beta j_y \quad (7)$$

Using the experimentally determined j_y and E_x in these equations, E_y and j_x were computed. As will be seen in Sec. 3, these computations clearly demonstrated that the present generator did not operate in the "shorted" mode.

3. MHD Generator Experimental Results

3.1 Initial Stagnation Gas Conditions

The initial experiments were at 6000°K stagnation gas temperatures. Subsequently, the temperature was gradually lowered toward 2000°K. The test gases consisted of argon, 50% helium + 50% argon, neon, 99% neon + 1% argon, and 99% neon + 1% xenon. The latter two mixtures exhibit ionization enhancement due to the Penning effect. The lowest temperatures at which large scale MHD power extraction was obtained were in the range of 3000–4000°K in the 99% neon + 1% xenon mixture. This gas mixture satisfied the two major requirements for successful generator operation; namely, a sufficiently high n_{eo} of about 10^{11} cm^{-3} in the stagnation region to achieve uniform preionization (see Sec. 3.2) and a sufficiently high $[(\mathbf{U} \times \mathbf{B})D]$ voltage to exceed the large electrode losses (see Sec. 3.4). The 99% neon + 1% xenon experiments were performed at two stagnation conditions. In the first case, the computed gas stagnation temperature, T_o, was 3650°K. The measured average stagnation pressure was 3.4 atm for the first 2 msec and 4.75 atm for the last 3 msec of the 5 msec test time. In the second case, the calculated T_o was 3950°K, and the measured stagnation pressures, P_o, were 1.25 atm for the first 2 msec and 1.8 atm for the last 2 msec of the 4 msec test time. The variation in the stagnation pressure during the test time was a result of operating the shock-tube in the "overtailored" mode.[5] "Overtailoring" also raises T_o. However, ultrasonic stagnation temperature measurements showed that T_o was within 10% of the aforementioned theoretical values. Since $T_e/T_o \approx 2$ in the present experiments, the exact value of T_o has only a minor effect on the generator operation. On the other hand, the generator performance is strongly affected by the ratio of the Lorentz force to the gas pressure. Consequently, in each experiment differences in generator behavior were observed as the stagnation pressure changed during the test time. Thus, to simplify the presentation, only the results obtained during the last 2 msec of the test time will be presented. Since the gas transit time through the generator was about 0.3 msec, quasi-steady state conditions generally existed during the 2 msec. In the rest of the paper, these two experimental conditions will be referred to as the T_o = 3650°K, P_o = 4.75 atm experiment and the T_o = 3950°K, P_o = 1.8 atm experiment.

3.2 Preionization Experiments

To achieve appreciable generator power output, uniform preionization at the generator entrance was necessary even if the stagnation electron density, n_{eo}, exceeded 10^{14} cm^{-3}. This was due to the large separation of 23 cm between the stagnation region and the generator entrance which resulted in large electron recombination. Reasonably uniform preionization was achieved by applying electrically isolated constant current sources to each of the seven preionization electrodes oriented parallel to the magnetic field and to each of the first 12 or 24 electrode pairs in the first four rows of the generator electrodes (see Fig. 1). The applied electric field at the latter electrodes was parallel to $\mathbf{U} \times \mathbf{B}$. It was observed that n_{eo} had to exceed about 10^{11} cm^{-3} to attain uniform preionization. The current at each of the first preionization electrodes was 30 amp, corresponding to a current density of 4 amp/cm^2, the interelectrode voltage was 310 v, and the power input was 70 kw for all gas conditions. The current was 5–20 amp at the second set of preionization electrodes, depending on the gas condition. At this second set of electrodes the power input ranged from 0 kw to 70 kw. Figure 2 shows the measured electron density in the MHD channel downstream of the preionization electrodes as a function of distance from the nozzle throat for the 99% neon + 1% xenon experiment at T_o = 3950°K and P_o = 1.8 atm. The theoretical curve shows the variation of n_e for the case where the magnetic field was zero. In computing the theoretical curves, the three-body recombination coefficient, $\alpha_R = 4.419 \times 10^{-17} T_e^{-5.56}$, m^6/sec, given by Dugan[13] was used. The four electron density measurements were about a factor of two above the theoretical curve. Since the plasma is nonuniform and the calibration of the photomultipliers is based on the assumption of a uniform plasma, it was decided to normalize the data point at x = 37 cm to the value given by the theoretical curve. All the other data points in Fig. 2 were divided by this normalization constant which was about 2. It can be seen that the points fall on the theoretical curve, and they thus verify Dugan's three-body recombination coefficient.

3.3 Open Circuit Generator Experiments

The voltage distribution in the generator at open circuit conditions is of considerable interest because severe current

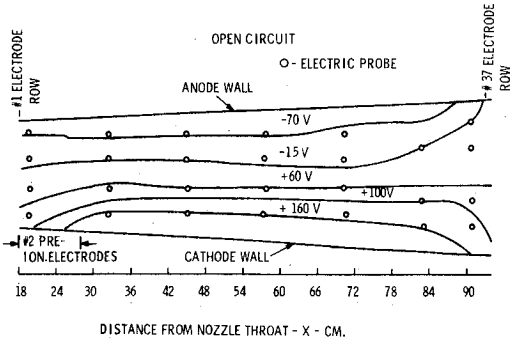

Fig. 3 Measured equipotential voltage distribution on the insulator wall at open circuit conditions for run 77 during the last 2 msec of the test time. Preionization was applied at both the first and second set of preionization electrodes. B decreased from 1.25 ± 0.05 Tesla at x = 18 cm to 0.89 ± 0.05 Telsa at x = 92 cm.

shorting has been observed in other experiments[8] at these conditions. The average potential distribution measured with the 24 flush mounted probes in the insulator wall (see Fig. 1) is shown in Fig. 3 for the $T_o = 3950°$K, $P_o = 1.8$ atm experiment. The magnetic field during this 2 msec part of the test time was 1.25 ± 0.05 Tesla, at the generator entrance. It decreased approximately linearly to 0.89 ± 0.05 Tesla at the generator exit. The open circuit experiments were performed with preionization at the channel entrance. Preionization was necessary because a minimum n_e in excess of 10^{13} cm^{-3} is required in the freestream to supply sufficient current to the electrostatic probes without altering the local plasma potential.[3] The presence of the preionization current can be detected in Fig. 3 in the region between $x = 18$ cm and $x = 28$ cm, where the second set of preionization electrodes are located and where the equipotentials are at an angle with respect to the channel axis. In the second region, extending from $x = 28$ cm to $x = 75$ cm, the equipotentials are approximately horizontal, as would be expected at open circuit. The average open circuit field in this region is 1860 ± 200 v/m. The theoretical $\mathbf{U} \times \mathbf{B}$ decreased from 2400 v/m at $x = 30$ cm to 2250 v/m at $x = 75$ cm. The slight decrease in $\mathbf{U} \times \mathbf{B}$ is caused by the fact that $\mathbf{U}$ increases in the downstream direction while $\mathbf{B}$ decreases. For $x > 75$ cm, the equipotentials are slanted with respect to the axis. The probable cause of the slanted equipotentials and of the 20% discrepancy between the measured and theoretical $\mathbf{U} \times \mathbf{B}$ in the central region of the channel is the low value of n_e in the channel (see Fig. 2). The freestream n_e in the downstream half of the channel is only about 10^{13} cm^{-3} which is in the threshold region at which accurate potential measurements can be obtained.[3] This latter explanation was verified by placing in the channel at $x = 75$ cm a pair of probes which protruded past the aerodynamic boundary layer. With the protruding probes open circuit $\mathbf{U} \times \mathbf{B}$ values were measured which were 10–35% higher than those obtained with the flush mounted probes at the same location. The aforementioned results show that the present generator does not have any appreciable internal shorting at open circuit conditions. This conclusion was also verified from the static pressure measurements along the insulator wall of the MHD channel. The static pressure distribution without a magnetic field or preionization was the same as with a magnetic field and preionization. If internal shorting exists at open circuit conditions, the equipotentials in the generator are slanted at about a 45° angle to the axis; and the pressure distribution differs considerably from that obtained in the absence of a magnetic field.[8]

3.4 Loaded Faraday Generator Experiments

3.4.1 Electrode conduction

In this section the operating characteristics of the 0.32-cm-diam copper electrodes and their influence on the generator performance will be given. The electrodes operated in the cold cathode, arc mode[2,3] in which the current flow to the electrode surface is concentrated in arc spots. The electrode ignition voltage was over 300 v; and the minimum discharge sustaining voltage (i.e., the combined anode and cathode voltage losses) was about 100 v. These voltage losses are caused primarily by the cold boundary layers, whose thickness ranged from 0.1–3 cm, and by the cold nonemitting electrodes. Electrode voltage losses of about the same magnitude were measured[14] under similar boundary layer conditions and in the absence of a magnetic field. Gas convective blowing of the discharge[2] produced an intermittent electrode current flow of about 20 kHz frequency. Due to the intermittent nature of electrode conduction, it was necessary to connect electrically isolated resistors to each of the 230 electrode pairs. For the same experimental conditions, the generator power output was about *twice as large* if each of the 230 electrode pairs were individually connected to a load resistor than if all the anodes or cathodes in each of 37 rows were electrically connected to a common point. Measurement of the current in each electrode pair of a few randomly selected rows showed that with individual load connections, the magnitude of the current was almost identical in each electrode pair. On the other hand, with the common load connection the current measurements showed that almost all the current in a row was carried by one electrode pair.

The maximum current per electrode was about 50 amp, or 500 amp/cm^2 if one assumes a uniform current distribution over the 0.32-cm-diam electrode. The actual current density at the electrode surface is considerably higher since the current flows through arc spots. A layer of carbon contamination developed on the electrode surface after a few runs. The source of the carbon was either vacuum pump oil vapors or arc induced erosion of the plastic insulating material around the electrode. Downstream of each cathode, a 0.3-cm-wide × 1-cm-long black track developed as a result of electrode current induced erosion of the plastic wall. The anodes were surrounded by a 1-cm-diam light black erosion on the insulator surface. No other erosion of the electrode or insulator wall could be detected even after 100 runs. The cathode erosion is in agreement with the theoretical current flow direction.[3] Since the electrode pitch was about 2.5 cm, current flow between neighboring electrodes along the electrode wall did not occur. Electrode contamination caused a rapid deterioration of the electrode current within a few hundred millisecond operating time. For example, experimental runs 76 and 132 were performed under identical conditions. In the former run, the total electrode operating time was 30 msec, and the generator power output was 480 kw; while in the latter one, the total operating was 200 msec, and the power was 200 kw. The electrodes were not cleaned between runs. This rapid deterioration of the electrodes due to carbon formation could be a possible explanation for the observed[15] rapid drop in the generator performance in a steady state experiment after about 100 msec. The cathode wall erosion could account for some of the internal shorting observed[8] in an MHD generator having a smaller axial electrode pitch than the present channel.

3.4.2 MHD generator electrical characteristics

The presentation of the results will be confined to two experiments performed in the 99% neon + 1% xenon mixture. In the first experiment, labeled run 73, T_o was 3650°K, P_o was 4.75 atm (see Sec. 3.1). In this case the electromagnetic-gas dynamic interactions were weak with $S = (\mathbf{U} \times \mathbf{B})L/(\rho U^2) < 0.1$. L is the total generator length. This experiment will be compared with experimental run 76 ($T_o = 3950°$K, $P_o = 1.8$ atm), where the electromagnetic-gas dynamic interactions were strong, with $(\mathbf{U} \times \mathbf{B})L/(\rho U^2) \approx 0.45$. In run 76 the strong MHD interactions produced a nonstationary shock wave in the generator. Both experiments were performed with individual load resistors, R_L, of 4Ω magnitude attached to each of the 230 electrode pairs. Experiments with R_L ranging for 1–10Ω showed that maximum generator power output was obtained in the vicinity of R_L equal to 4Ω.

Figure 4 shows the measured transverse generator current, j_y, for run 73, while Fig. 5 shows j_y for run 76. In run 73, the rate of current growth at the front of the generator is considerably slower than in run 76. This is due to the higher pressure in run 73, which reduces the ionization rate below that attained in run 76. While j_y remains at a fairly high level in run 73 (Fig. 4), the generator current cuts off near the downstream end of the generator in run 76 (Fig. 5). As will be shown below, the current cutoff can be attributed to the presence of a shock-wave. The solid curves in Figs. 4 and 5 were used as input quantities in the numerical analyses of the generator performance.

Figures 6 and 7 show the equipotential voltage distribution, measured on the insulator wall, for runs 73 and 76, respec-

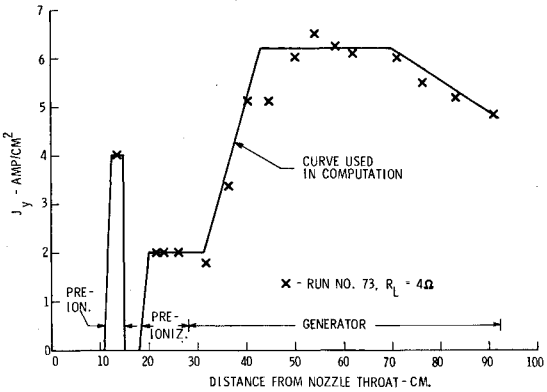

Fig. 4 Experimental current density variation (based on the total electrode wall area) along the generator for run 73 during the last 3 msec of the test time. T_o = 3650°k and P_o = 4.75 atm. R_L equalled 4 Ω per electrode pair. The curve shown in the figure was used as an input quantity in the analyses.

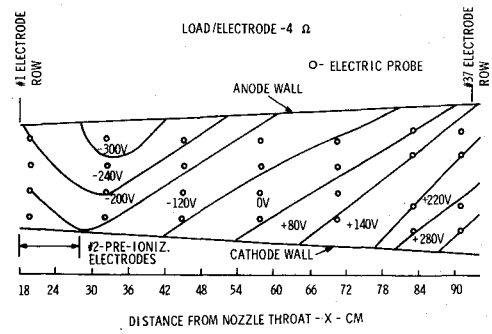

Fig. 6 Measured equipotential voltage distribution on the insulator wall for run 73 during the last 3 msec of the test time.

tively. In Fig. 6 the slope of the equipotentials changes direction at about x = 30 cm. This indicates that the axial Hall field, E_x, reverses direction at about x = 30 cm and that a current loop exists at that location near the anode wall. No E_x reversal occurred in run 76 (Fig. 7). However, the equipotentials are almost perpendicular to E_x near the anode wall at the exit and entrance, indicating the possible presence of axial end currents. The explanation for the E_x reversal is as follows: The MHD generator is insulated from ground potential for a distance of about 150 cm downstream of the generator exit and for a distance of 18 cm upstream of the generator entrance. Initially, the plasma at the generator entrance is at ground potential, and the plasma downstream of the generator is at a positive potential equal to the Hall voltage at the generator exit. When the downstream plasma comes in contact with ground potential, the potential distribution in the generator shifts, with the zero voltage line moving upstream. Thus, to satisfy the ground potential requirement upstream of the generator entrance, the Hall field must reverse itself. Since in run 73 (Fig. 6) the negative potential is higher at x = 18 cm than in run 76 (Fig. 7), the E_x reversal point in the former case is further upstream. This explanation was verified when it was observed that the zero voltage line in the generator abruptly shifted upstream about 1 msec after the start of the test time. One msec is the time it takes the gas to flow from the generator exit to the downstream grounded part of the facility. A second point of interest is that for $x > 32$ cm in Fig. 6, the equipotentials are reasonably straight indicating that no large scale internal current loops exist in the core of the flow. Such loops were observed[8] in a generator operating in the "shorted" mode in which large axial Hall currents flowed inside the generator. Close to the electrode walls the potential distribution is different from that shown in the figures due to electrode voltage losses. However, no current loops exist near the walls since the Hall voltage, measured at the electrodes, increased monotonically for $x > 30$ cm. The final point of interest is the observation that in run 76 (Fig. 7) the equipotentials become nearly horizontal for 72 cm $< x <$ 90 cm. This indicates an absence of transverse current, which is in agreement with the measured j_y at this location (see Fig. 5).

Figure 8 shows the computed and measured E_x and E_y fields for run 73. The "plasma turbulence" model with $\xi = 1$ was used in the computation with the j_y curve in Fig. 4 as an input quantity. The experimental points were taken from the equipotential plot in Fig. 6, and they have an accuracy of about ±15%. The E_y values agree fairly well with computation. For $x > 45$ cm, E_x is in semiquantitative agreement with the computed field. For $x < 45$ cm, the E_x values disagree because the analyses did not include the effect of end shorting (see Fig. 6). Figure 9 shows the experimental and computed Hall field for run 76 obtained with the j_y curve in Fig. 5. This figure clearly shows that the "plasma turbulence" model gives the best agreement with the measured Hall field. Also, since E_x did not reverse in the generator in this experiment (see Fig. 7), the experimental result is in good agreement with the computation along the entire channel. Figure 10 shows the E_y field for run 76. For $x <$ 40 cm, the measured values are in good agreement with the "plasma turbulence" model. For $x > 40$ cm, the computations disagree. As will be shown later, the disagreement is due to the presence of a shock-wave which was not included in the calculation. The agreement of the experimental results with the "plasma turbulence" model with a ξ of 1 implies that β_{EFF} is about 1 and that the plasma was highly turbulent. In the small shock-tube experiments,[1-3] the measured β_{EFF} was between 2 and 3 for $\beta > 2$. The higher effective Hall parameter in the latter experiments could possibly be due to the stabilizing effect of the channel walls on the discharge structure in the generator. The wavelength of the plasma nonuniformities was about 3 cm,[2] whereas the channel width was

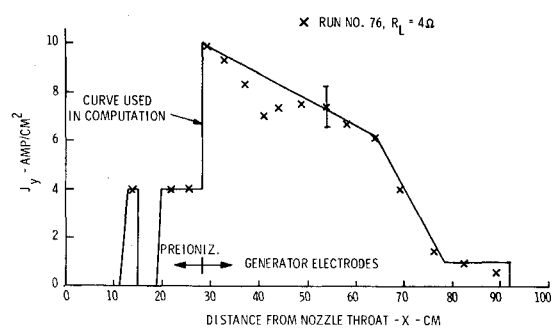

Fig. 5 Experimental current density variation along the generator for run 76 where T_o = 3950°k and P_o = 1.8 atm. R_L = 4Ω/electrode.

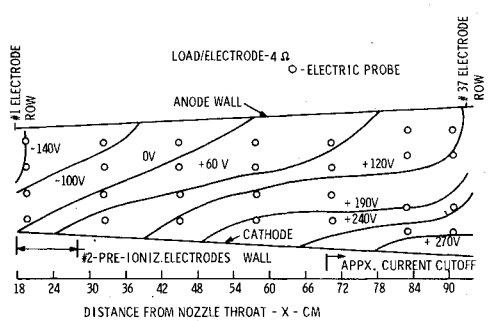

Fig. 7 Measured equipotential voltage variation on the insulator wall for run 76 during the last 2 msec of the test time. The approximate point of current cutoff (see Fig. 5) is shown at x = 70 cm.

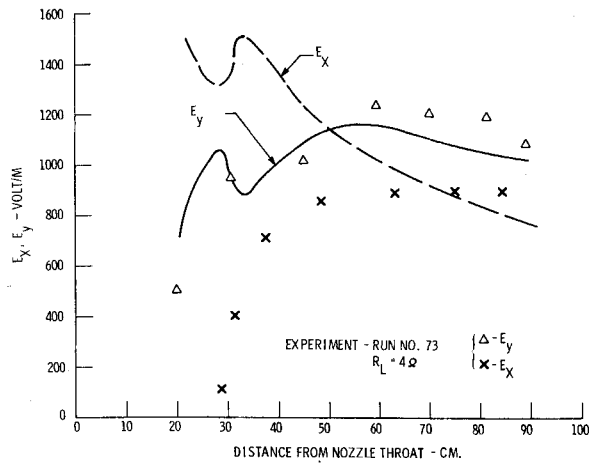

Fig. 8 Computed and experimental transverse and axial electric field variation along the generator for run 73 during the last 3 msec of the test time. The "plasma turbulence, $\xi = 1$" conductivity model was used to compute the Hall field, E_x, and transverse electric field, E_y, curves.

5 cm in the small shock-tube and an average of 20 cm in the present facility. Thus, the assumption of homogeneous turbulence is only appropriate in the present experiments. Finally, the electrical performance for runs 73 and 76 was computed using the "shorted" mode calculation [Eqs. (6) and (7)]. It was found that the computed E_y would be about 100 v/m, and the generator power output would be about zero if the generator operated in the "shorted" mode. A low E_y implies large ohmic dissipation in the plasma, and this is a characteristic of an internally shorted generator.[3]

3.4.3 *MHD generator plasma properties*

Figure 11 shows the measured and computed electron density in the generator for run 76 (T_o = 3950°K, P_o = 1.8 atm). The data points were normalized by the same factor used for the preionization experiments in Fig. 2. With the exception of the measurement at the generator exit, the data lies between the "plasma turbulence" and "finite electrode" calculation. The agreement with the former model is considered satisfactory in view of the large fluctuations in the measured radiation signals. The higher n_e at the exit, x = 92 cm, could be due to end currents whose existence was deduced from the potential measurements (Fig. 7). From the "plasma" turbulence" model one obtains an average T_e of 7000° ± 1000°K in the region, 30 cm < x < 70 cm, where j_y

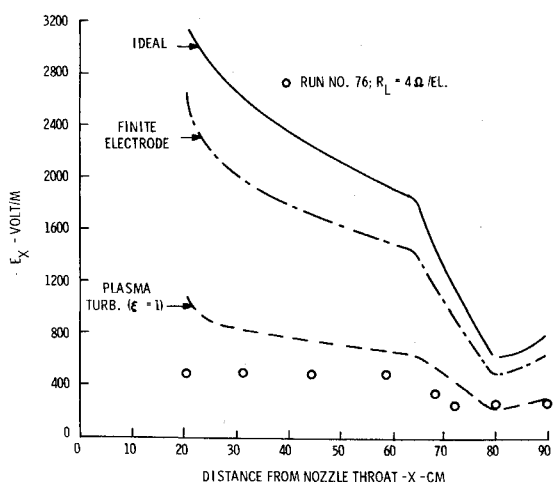

Fig. 9 Computed and experimental Hall field variation along the generator for run 76 during the last 2 msec of the test time.

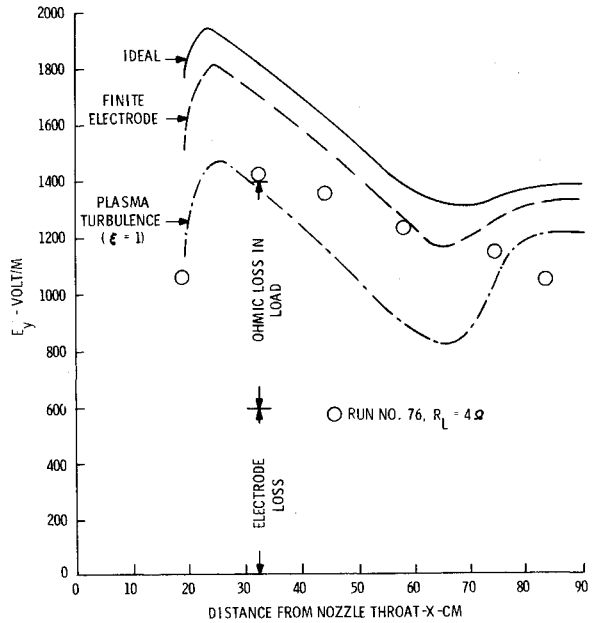

Fig. 10 Computed and experimental transverse electric field variation along the generator for run 76 during the last 2 msec of the test time.

is a maximum (Fig. 5). For 30 cm < x < 70 cm, the computed T_e is 2100 ± 100°K, σ is about 400 mho/m, and β ranges from 5 at the front of the generator to 9 near the exit.

3.4.4 *MHD generator gas dynamic characteristics*

The gas dynamic characteristics for runs 73 and 76 are given in Figs. 12 and 13, respectively. For comparison purposes, the open-circuit measurements obtained in run 77 are also shown in both figures. In run 73 the total interaction parameter, S, was 0.13 which is relatively low. Figure 12 shows that excellent agreement exists between the experimental and computed static pressure distributions for run 73 and run 77. By using a stagnation pitot tube, the Mach

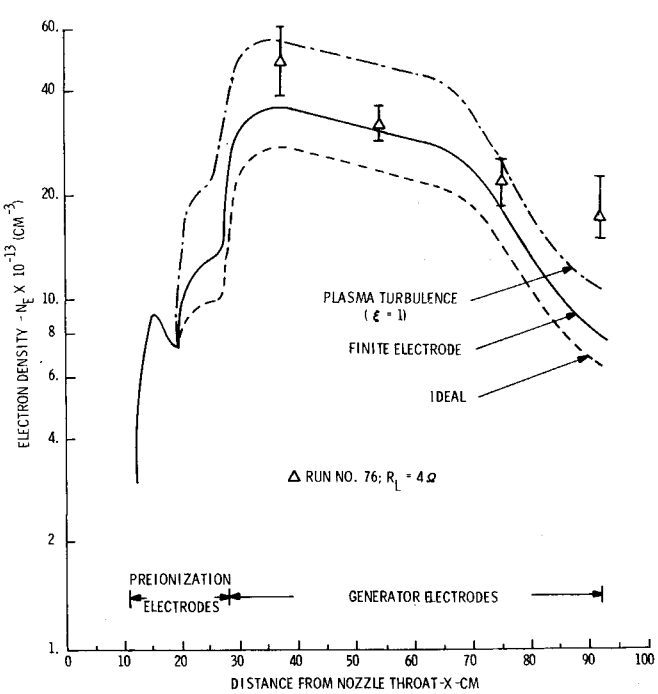

Fig. 11 Computed and experimental electron density variation along the generator for run 76 during the last 2 msec of the test time.

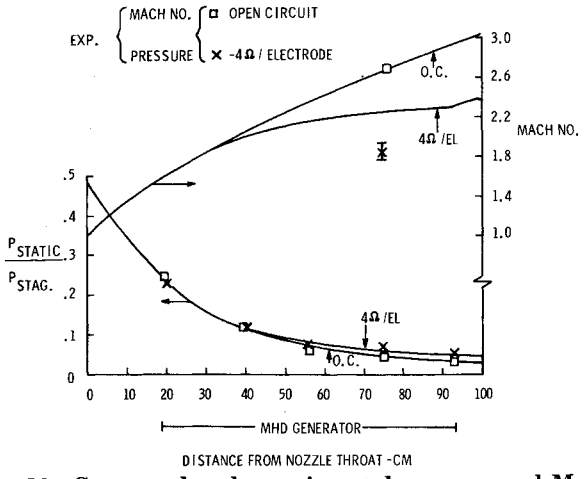

Fig. 12 Computed and experimental pressure and Mach number variation along the generator for run 73 during the last 3 msec of the test time.

number in the channel was obtained. In run 77 the measured Mach number is in reasonable agreement with the computed value. Strong pressure fluctuations were recorded in the piezoelectric transducer in the pitot tube, especially in the presence of the generator current. Of the many measurements only those at $x = 75$ cm were sufficiently repetitive to be useful. Consequently, the 20% discrepancy between the measured and computed Mach numbers in run 73 is not surprising. It is to be noted that in computing the theoretical generator performance for runs 73 and 76, the "plasma turbulence" conductivity model was used. This model produces higher ohmic dissipation and entropy increases than the "ideal" case, and it thus results in a higher static pressure and temperature and lower Mach number. For run 73 the difference in the gas dynamic properties between the two conductivity models is negligible, while for run 76 it was less than 10%. In run 76 the computed total interaction parameter, S, based on the total generator length, was 0.45. Under this strong interaction condition a normal shock wave in the generator could be expected. The static pressure signal at

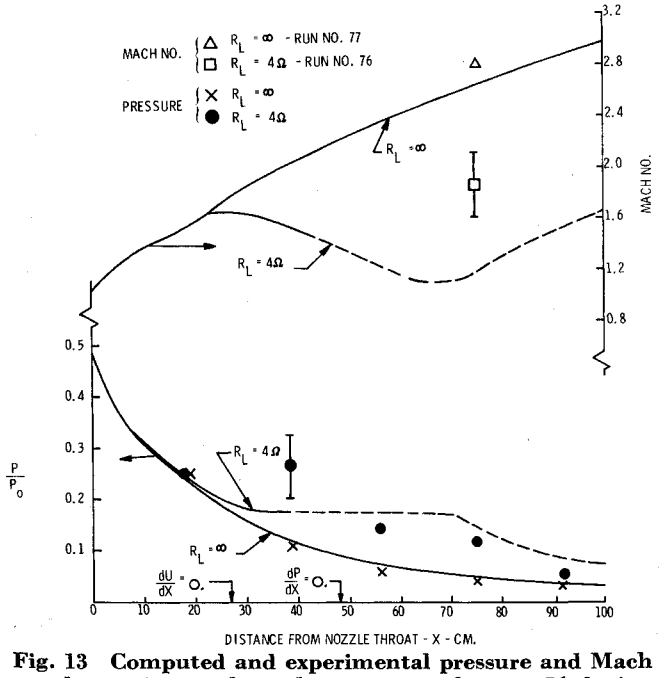

Fig. 13 Computed and experimental pressure and Mach number variation along the generator for run 76 during the last 2 msec of the test time.

Table 1 Theoretical and experimental generator performance for 99% neon + 1% xenon: $T_o = 3950°K$, $P_o = 1.8$ atm

	A) Heat input kw	B) MHD power output kw	Generator turbine efficiency	Generator Conversion efficiency $= A/B$
Theory:				
Normal mode: Ideal	5800	1556	81%	27%
Normal mode: Plasma turbulence	5800	1090	56%	19%
Shorted mode	5800	100	≈0%	≈0%
Experiment:				
Power output	5800	430	26%	7.5%
Power output + electrode loss (≈120v)		930	56%	16%

$x = 38$ cm, where $S = 0.10$, shows the existence of a strong pressure disturbance, indicating the presence of a shock wave. The error flag at this point shows the range of pressure variation during the 2 msec of the test time under consideration. At all the other points, the pressure, P, was relatively constant during the 2 msec period. The theoretical computation showed that dP/dx changed slope at $x = 48$ cm, and dU/dx changed slope at $x = 27$ cm. In combustion MHD generator experiments[16] it was observed that a normal shock wave existed in the vicinity of the location where dP/dx changed sign. To determine if a stationary shock could exist between $x = 27$ cm and $x = 48$ cm, the Rankine-Hougoniot equations were introduced into the computations at $x = 30$ cm and at $x = 48$ cm. In both cases the computation showed that the flow remained subsonic until the generator exit at $x = 92$ cm. Since the generator exit Mach number must be unity to match the low pressure condition in the expansion tank of the shock-tunnel, a stationary solution with a normal shock in the generator is not possible. Indeed, the strong time dependence of the pressure at $x = 38$ cm indicates that the shock-wave is nonstationary. It is not clear whether the shock is normal or oblique. The theoretical pressure and Mach number variations for $x > 38$ cm are shown as dashed curves to indicate the nature of the shock-free solution. The agreement of the pressure curve with the measured values for $x > 38$ cm is probably coincidental. The shock-wave lifts and thickens the boundary layer. This would increase the electrode voltage loss, and it could account for the current cutoff in run 76 near the downstream end of the generator (see Fig. 5).

3.4.5 Over-all MHD generator performance

Table 1 summarizes the over-all generator performance as predicted by the various conductivity models and as experimentally observed for run 76, where $T_o = 3950°K$, $P_o = 1.8$ atm and $R_L = 4\ \Omega$/electrode. As a measure of the magnitude of the energy extraction of the generator, we define a conversion efficiency as the ratio of the electrical power output divided by the thermal input power. The generator turbine efficiency is the net MHD power output divided by the isentropic change in stagnation enthalpy between the generator entrance and exit stagnation pressure. The table clearly shows that the generator did not operate in the "shorted" mode since the power output would have been zero. The primary difference between the "ideal" generator performance and the "plasma turbulence" result is that the entropy increase is greater in the latter. Thus, the generator turbine efficiency, which is the crucial parameter determining the feasibility of the MHD Brayton cycle, is considerably lower in the "plasma turbulence" case. In run 76 the total gener-

ator output was 500 kw gross and 430 kw net. The 70 kw difference is due to the preionization power. If the electrode voltage loss of 120 v could be recovered by use of hot, emitting electrodes, the 930 kw net power would be in close agreement with the computed values. Also, the generator turbine efficiency would be increased from 26% to 50%. It is interesting to note that the minimum turbine efficiency required for a Brayton cycle is about 60%.[17]

4. Conclusions

The following major conclusions can be drawn from this study: 1) Uniform preionization at the generator entrance was required to attain large scale electrical power extraction, irrespective of the stagnation electron density. The preionization power was less than 10% of the maximum generator output power. 2) Electrode voltage losses and shock-wave formation were the two major factors limiting the generator power. Of about 1 mw electrical power delivered to the electrode wall, which equaled about 17% of the thermal power, about 50% was dissipated internally at the electrodes. The shock-wave, by thickening the boundary layer, further increased electrode losses to values approaching the open circuit voltage. The shock-wave was located within 10 cm of the location where the slope of dU/dx changed sign. Thus, improved generator performance would result if emitting electrodes which protrude past the boundary layer were used and if the channel geometry were redesigned to eliminate adverse velocity or pressure gradients. 3) Perhaps, the most significant result of this study was that the electrical performance of this generator was essentially similar to that of the small shock-tube MHD generator, even though the channel volume was 50 times larger. The only difference was that the effective Hall parameter of unity was about one-half the value in the small generator. The lower effective Hall parameter in the large channel was attributed to the reduced influence of the channel walls on the discharge structure. Consequently, a uniform turbulence conductivity model could be used to adequately describe the generator electrical performance. One would, therefore, expect that the present results could be applied to much larger MHD channels.

References

[1] Zauderer, B., "Experimental Study of Non-Equilibrium Ionization in a Linear MHD Generator," *AIAA Journal*, Vol. 6, No. 4, April 1968, pp. 701–709.

[2] Zauderer, B., "Discharge Structure and Stability of a Non-Equilibrium Plasma in a MHD Channel," *The Physics of Fluids*, Vol. 11, No. 12, Dec. 1968, pp. 2577–2585.

[3] Zauderer, B. and Tate, E., "Electrical Characteristics of a Linear Non-Equilibrium MHD Generator," *AIAA Journal*, Vol. 6, No. 9, Sept. 1968, pp. 1685–1694.

[4] Zauderer, B. and Tate, E., "Interaction of an Incident Shock Tube Flow with an Electromagnetic Field, Part II—Experiment," *Proceedings of the Seventh International Shock Tube Symposium*, Univ. of Toronto, Toronto, Canada, 1970, pp. 490–505.

[5] Zauderer, B. and Tate, E., "A Large Scale Non-Equilibrium MHD Generator," *Electricity from MHD*, Vol. II, International Atomic Energy Agency, Vienna, Austria, 1968, pp. 807–824.

[6] Zauderer, B. and Tate, E., "Performance of a Large Scale Non-Equilibrium MHD Generator with Rare Gases," TIS 70SD4, March 1970, General Electric Co., King of Prussia, Pa.

[7] Jackson, W. D., ed., "MHD Electrical Power Generation, The 1969 Status Report," April 1969, International Atomic Energy Agency, Vienna, Austria.

[8] Reilly, J. P., "Open and Short Circuit Experiments with a Non-Equilibrium MHD Generator," *Proceedings of the Tenth Symposium on Engineering Aspects of MHD*, Massachusetts Institute of Technology, Cambridge, 1969, pp. 158–171.

[9] Bertolini, E., Toschi, R., and McNab, I. R., "Relaxation Phenomena in MHD Generators," *Electricity from MHD*, Vol. I, International Atomic Energy Agency, Vienna, Austria, 1966, pp. 533–545.

[10] Zauderer, B., "Measurement of the Electrical Conductivity of Xenon in a Shock Tube," *AIAA Journal*, Vol. 8, No. 4, April 1970, pp. 645–648.

[11] Zampaglione, V., "Effective Conductivity of an MHD Plasma in a Turbulent State," *Electricity from MHD*, Vol. I, International Atomic Energy Agency, Vienna, Austria, 1968, pp. 593–604.

[12] Kerrebrock, J. L., "Segmented Electrode Losses in MHD Generators with Non-Equilibrium Ionization," *AIAA Journal*, Vol. 4, No. 11, Nov. 1966, pp. 1938–1947.

[13] Dugan, J. V., Jr., "Three-Body Collisional Recombination Coefficient for Cesium and Argon Ions," *Journal of Applied Physics*, Vol. 37, No. 13, Dec. 1966, pp. 5011–5012.

[14] Zelikson, Yw. M., Kirillov, V. V., Reshetov, E. P., and Flid, B. D., "Laws Governing the Operation of Metallic Electrodes in an MHD Generator," *Teplofizika Vysokikh Temperatur*, Vol. 8, No. 1, Jan. 1970, pp. 193–202; also *High Temperature*, Vol. 8, No. 1, Jan. 1970, pp. 181–189.

[15] Zettwoog, P., "Experimental Results in Hall Generators at 1600°K," *Proceedings of the Tenth Symposium on Engineering Aspects of MHD*, Massachusetts Institute of Technology, Cambridge, p. 109, 1969.

[16] Louis, J. F. and Brogan, T. R., "Fluid Mechanics in MHD Generators," *Proceedings of the Second International Symposium on MHD Electrical Power Generation*, Vol. III, European Nuclear Energy Agency, Paris, 1964, pp. 1413–1424.

[17] McNab, I. R., Rapporteur on "Power Plant Concepts and Economies," *Electricity from MHD*, Vol. VI, International Atomic Energy Agency, Vienna, 1968, pp. 3637–3648.